5-12-2022

Prediction and confirmation of a switch-like region within the N-terminal domain of hSIRT1

Angelina T. Huynh
San Jose State University, angelinatienhuynh@gmail.com

Thi-Tina N. Nguyen
San Jose State University

Carina A. Villegas
San Jose State University

Saira Montemorso
San Jose State University

Benjamin Strauss
San Jose State University, benjamin.strauss@sjsu.edu

See next page for additional authors

Recommended Citation

Authors

Angelina T. Huynh, Thi-Tina N. Nguyen, Carina A. Villegas, Saira Montemorso, Benjamin Strauss, Richard A. Pearson, Jason G. Graham, Jonathan Oribello, Rohit Suresh, Brooke Lustig, and Ningkun Wang

Prediction and confirmation of a switch-like region within the N-terminal domain of hSIRT1

Angelina T. Huynh [a,1], Thi-Tina N. Nguyen [b,1], Carina A. Villegas [b,1], Saira Montemorso [a], Benjamin Strauss [c], Richard A. Pearson [a], Jason G. Graham [d], Jonathan Oribello [a], Rohit Suresh [a], Brooke Lustig [a,**], Ningkun Wang [a,*]

[a] *Department of Chemistry, San José State University, San José, California, 95192, USA*
[b] *Department of Biological Sciences, San José State University, San José, California, 95192, USA*
[c] *Department of Computer Science, San José State University, San José, California, 95192, USA*
[d] *Department of Biomedical, Chemical, and Materials Engineering, San José State University, San José, California, 95192, USA*

ABSTRACT

Many proteins display conformational changes resulting from allosteric regulation. Often only a few residues are crucial in conveying these structural and functional allosteric changes. These regions that undergo a significant change in structure upon receiving an input signal, such as molecular recognition, are defined as switch-like regions. Identifying these key residues within switch-like regions can help elucidate the mechanism of allosteric regulation and provide guidance for synthetic regulation. In this study, we combine a novel computational workflow with biochemical methods to identify a switch-like region in the N-terminal domain of human SIRT1 (hSIRT1), a lysine deacetylase that plays important roles in regulating cellular pathways. Based on primary sequence, computational methods predicted a region between residues 186–193 in hSIRT1 to exhibit switch-like behavior. Mutations were then introduced in this region and the resulting mutants were tested for allosteric reactions to resveratrol, a known hSIRT1 allosteric regulator. After fine-tuning the mutations based on comparison of known secondary structures, we were able to pinpoint M193 as the residue essential for allosteric regulation, likely by communicating the allosteric signal. Mutation of this residue maintained enzyme activity but abolished allosteric regulation by resveratrol. Our findings suggest a method to predict switch-like regions in allosterically regulated enzymes based on the primary sequence. If further validated, this could be an efficient way to identify key residues in enzymes for therapeutic drug targeting and other applications.

1. Introduction

Allosteric regulation has been known to play an important role in tuning protein function since the conception of the Monod-Wyman-Changeux (MWC) model in 1965 [1]. With the advancement of biochemical and biophysical techniques, it has become apparent that the allosteric phenomena, where an effector ligand binding at a distal site can regulate certain protein functions through long-distance communication, are wide spread among many proteins, ranging from enzymes to receptors [2–4]. Allosteric communication is made possible through the flexibility of proteins [5]. These changes in protein dynamics can be manifested through a continuum of conformational changes ranging from local residue movements to global fluctuations [6,7]. Often a few key residues play a critical role in transducing the binding of the allosteric molecule. Locating these key residues could be powerful in aspects of understanding the molecular mechanism of the allosteric

communication or drug targeting. In many cases, these switch-like regions tend to be flexible stretches of amino acids that undergo a change in secondary structure or peptide backbone conformation upon binding an allosteric modulator [6,8–11]. Identifying specific residues or short regions crucial to allosteric responses, termed allosteric switch-like regions or nodes, have been of intense interest in the field [6,9]. As it could be arduous to experimentally identify switch-like regions through routine mutation scanning, various computational approaches have been pioneered to predict switch-like regions [10,12,13]. These approaches, however, oftentimes require detailed structural information and intensive computational power.

One such protein with an important allosteric system is SIRT1, a mammalian NAD^+-dependent lysine deacetylase that undergoes allosteric regulation. Many proteins have been identified as substrates for SIRT1, implicating its involvement in important cellular pathways, including glucose metabolism, cellular apoptosis and

neurodegeneration [14–16]. SIRT1 is a two-domain enzyme that undergoes interdomain allosteric regulation [17,18], which includes a structured catalytic core [19] that is highly conserved in the Sirtuin family [20] and flanking N- and C-terminal domains that are partially unstructured and potentiate deacetylase activity [21,22]. Several small molecules that allosterically increase SIRT1 activity have been studied, termed sirtuin activating compounds (STACs) [23]. Crystal structures of SIRT1 bound to STACs such as resveratrol have shown that the small molecule STAC binds the three-helix bundle STAC binding domain (SBD) that is far away from the substrate binding sites in the catalytic core (Fig. 1B). The SBD is especially important for enzyme activity and STAC-dependent regulation [24–26]. Regulating the activity of SIRT1 has been explored as a therapeutic approach for treating diseases such as Alzheimer's disease and diabetes [27]. However, while E230 has been identified as a direct binding site for STACs, no allosteric switch region has been confirmed.

Here we use human SIRT1 as a testing candidate to develop and implement a more accessible and universal computational method for identifying *de novo* switch-like regions independent of the function or structure of the protein, using a series of descriptors based on primary sequence [28]. The characterization of structurally ambivalent sequence elements utilized secondary structure propensities which were determined from sequence [29]. More explicitly, regions with inaccurately predicted secondary structure features were found to be a good preliminary marker of such key switch-like regions [30]. Sequence entropy has been shown to be a useful marker for ambivalent secondary structure features as well as possible residue disorder propensity [31]. An extensive set of such descriptors were previously shown to be predictive for solvent accessibility via logistic regression [28], a property related to potential switch-like behavior [32]. We adapted our logistic regression approach to the characterization of ambivalent secondary structure features using *N*-acetyl transferases, a system that has particularly well-characterized switch-like regions, as a learning set and then applied it to sirtuins ([33] and unpublished data). The results show that the best models involved three sequence descriptors: secondary structure variability (V_{kabat}), 6-term sequence entropy (E6), and Lobanov-Galzitskaya disorder propensity (IsUnstruct).

In this study we use a well-studied STAC, resveratrol, to test the allosteric switch-like regions in hSIRT1 that were predicted based on these sequence descriptors as overviewed in Fig. 1A. If the predictions are correct, abolishing the switch-like properties in the predicted regions would result in a hSIRT1 construct that is still active, but no longer responds to regulation by resveratrol. In this way, we were able to predict and confirm a single switch-like residue within the SBD of hSIRT1.

2. Materials and methods

Please see SI for additional details for the methods.

2.1. Calculation of sequence descriptors

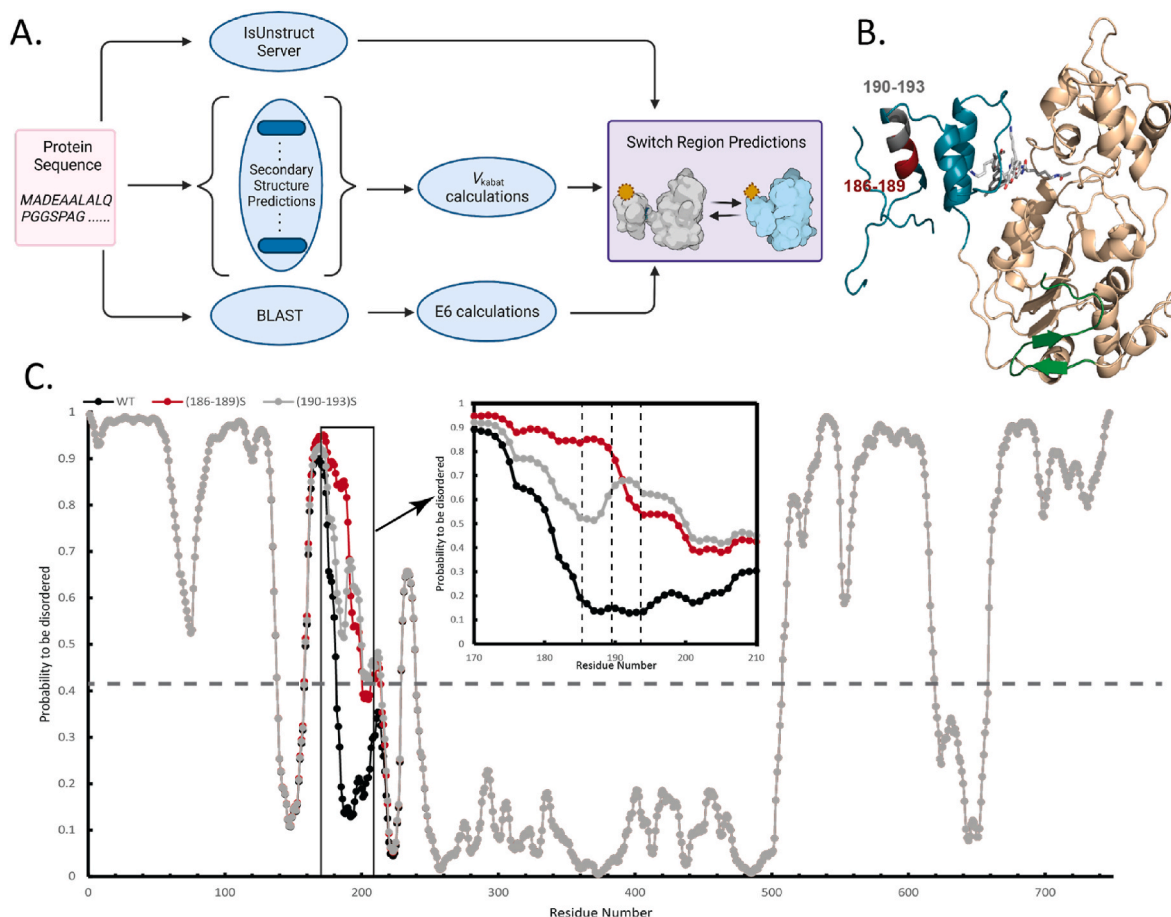The residue disorder propensity (IsUnstruct) was calculated using

Fig. 1. A. Brief computational workflow for switch-like region prediction. Created with BioRender.com. **B.** Structure of hSIRT1 (PDB ID 4ZZJ) including the catalytic core (tan), the ESA (green), and the SBD (teal). A substrate peptide (light gray) and a STAC compound (dark gray) is also shown. Predicted switch-like regions 186–189 (red) and 190–193 (gray) are highlighted **C.** Disorder prediction results of WT hSIRT1 (black), hSIRT1(186–189)S (red) and hSIRT1(190–193)S (gray). Results for the residues containing the predicted switch-like region is highlighted in the insert. (For interpretation of the references to colour in this figure legend, the reader is referred to the Web version of this article.)

IsUnstruct v2.02 [34]. The secondary structure variability (V_{kabat}) was estimated by a set of 15 prediction algorithms [35]. The sequence entropy and disorder (E6) at a given residue position was calculated over the six classes of amino acids [36].

2.2. Protein expression and purification

Human SIRT1 constructs were expressed as His-SUMO-tagged proteins in the BL21(DE3) strain of *Escherichia coli* using a pET28a-smt3 vector. The protein was purified by Ni-NTA affinity chromatography followed by cleavage of the SUMO tag and further purification by size exclusion chromatography, purity confirmed by SDS-PAGE and concentration determined by Bradford and BCA assays.

2.3. Enzyme-coupled assays for hSIRT1 activity

hSIRT1 activity was measured using a previously published continuous enzyme-coupled assay [37]. Peptide substrates were 11 or 13-mer peptides with the acetylated-lysine at the middle position. Kinetic parameters were obtained by fitting the initial rates to the Michaelis-Menten equation in GraphPad Prism.

2.4. Circular dichroism (CD) of hSIRT1 proteins

CD spectra were collected on an AVIV Model 215 Circular Dichroism Spectrometer. Secondary structure estimation was completed using the K2D3 method [38]. The melting curve of the hSIRT1 constructs were obtained by a temperature scan from 25 °C to 95 °C at 222 nm. The melting temperature was fitted using the Boltzmann Sigmoidal fit in GraphPad Prism.

3. Results

3.1. Predicting a switch-like region within the SBD of hSIRT1

A region between residues 186–193 within hSIRT1 was determined to exhibit switch-like behavior. Three associated descriptors, 6-term sequence entropy (E6), Lobanov-Galzitzskaya disorder propensity (IsUnstruct) and variability in predicted secondary structure (V_{kabat}) are associated with the better performing models for prediction of individual switch residues via logistic regression. These entailed a learning set of 48 N-acetyltransferases applied to a test set of five sirtuins, 2B4YA, 2HJHA, 4IG9A, 4L3OA, and 5BTRA. Descriptor overlays for 5BTRA indicated regions consistent with typically considered lower E6 (<60th percentile) [39], IsUnstruct (<40th percentile) [40] and high V_{kabat} (>85th percentile) [41] values. Regions of interest are at minimum triplets that have these percentile thresholds. Additional analysis exploring secondary structure variability for 3D-model structures was used to filter out less-likely regions and rank high-probability regions. Model structures were generated via I-TASSER, C-I- TASSER, RaptorX-Deep Learning, and Robetta for the complete hSIRT1 sequence. Filtering criteria was established by statistical analysis of the protein's XSSP-DSSP derived V_{kabat} and other values. By comparing the remaining regions' mean V_{kabat} values, they were ranked highest-to-lowest in the following order: 295–298, 186–193, and 447–452. Residues 186–193 reside in the SBD (Fig. 1B), hence, we focused on this segment as a potential switch-like region for SIRT1 allosteric regulation by STACs.

Experimentally mutating these residues to different amino acids individually would be time-consuming. Therefore, we used the sequence disorder propensity descriptor to help narrow down which amino acid mutations would no longer exhibit switch-like properties. Residues 186–189 and 190–193 were replaced with four of the same amino acids respectively, and the sequence disorder propensity was calculated for the resulting mutated sequence. This replacement prediction was carried out with all 20 amino acids. Ultimately, a replacement with four serines in either 186–189 or 190–193 resulted in drastically higher sequence disorder propensities (Fig. 1C). These mutations also resulted in significantly lowered V_{kabat} values at certain residues (Table 1). Together the results suggest that these mutations would abolish the switch-like property of these regions. Comparisons of the sequence descriptor values for similar 4-mer substituted serine mutants (including overlapping sets) for regions 295–298 and 447–452 showed patterns comparable to region 186–193 (Tables S2–S7), with the most significant changes involving increased IsUnstruct values and more moderate decreases for V_{kabat} values.

3.2. Experimental verification of a switch-like region in SIRT1

The computational results suggested that residues 186–193 had switch-like properties, and replacing the residues with serines would abolish this property. We chose to use resveratrol, a known allosteric regulator, as a tool to perturb the hSIRT1 system and test for the preservation or loss of the allosteric network. If our prediction was accurate, mutating the identified residues into serines would result in a mutant hSIRT1 that still retained activity, but was no longer allosterically regulated by resveratrol.

For the biochemical studies we used a truncated, more stable hSIRT1-143 construct [17] which has been shown to display similar activity as full length hSIRT1 and has been used for studies on resveratrol-based allosteric effects involving the N-terminal region [25]. The sequence descriptor values of residues 186–193 in the hSIRT1-143 construct did not show any significant difference between the those from full length hSIRT1 construct before or after the serine mutations, suggesting that the allosteric switch-like property is still retained in the truncated hSIRT1-143 construct (Figs. S1–S2, Table S1). All enzyme kinetics were obtained through a continuous enzyme-coupled assay [37] using acetylated peptide substrates without any attached fluorophore. This was to ensure that the results were not affected by the artifact of resveratrol having an affinity to aromatic fluorophores such as 7-amino-4-methylcoumarin [42].

We started out by testing the residues in broad strokes, introducing 4-serine mutations to residues 186–189 and 190–193, termed hSIRT1-143 (186–189)S and hSIRT1-143 (190–193)S. Once a large region was confirmed as the switch-like region, we would then hone in on that region to identify a single residue as the switch. Both hSIRT1-143 (186–189)S and hSIRT1-143 (190–193)S were successfully expressed and purified (Fig. S3). WT and mutant SIRT1 constructs all presented as monomers by SEC analysis, consistent with that observed in previous literature [43] (Fig. S4). The mutants had slightly lower melting temperatures (Table 1 and Fig. S5), but CD spectra of the two mutants reflected a well-folded protein with both α-helical and β-sheet secondary structure components [38], similar to that of WT hSIRT1-143 (Fig. 2A and Table S8). Computational docking studies suggest that the binding energy for the mutants and resveratrol were not dramatically changed [44] (Table S9), and fluorescence-based binding studies showed that while the binding affinity of resveratrol to the mutant hSIRT1-143 constructs decreased (Fig. S6), the amount of resveratrol added in the enzymatic assays ensured that at least 80% of hSIRT1 mutant proteins were still bound to resveratrol. Importantly, the mutants exhibited activity towards a known peptide substrate of hSIRT1, Ac-H3 [37] (Fig. S7, Table S10).

We then quantified the activity of different hSIRT1 constructs towards Ac-p53W with and without resveratrol. Without resveratrol, the hSIRT1 mutants showed overall lower activity against Ac-p53W. The k_{cat} values were significantly decreased in both mutants, while the K_M values were not statistically different between the mutants and WT hSIRT1-143. Inspection of the hSIRT1-143 structure reveals that V188 in the first helix (H1) possibly has hydrophobic interactions with V224 and I225, two residues in the third helix (H3) within the SBD (Fig. 3). The mutation of V188 to serine would disrupt this hydrophobic interaction and likely result in the destabilization of the three-helix bundle [45], which has been shown to decrease the catalytic rate of hSIRT1 [46]. In

Table 1
Sequence descriptor values for residues 186–193 for both WT hSIRT1 and the four-serine mutations.

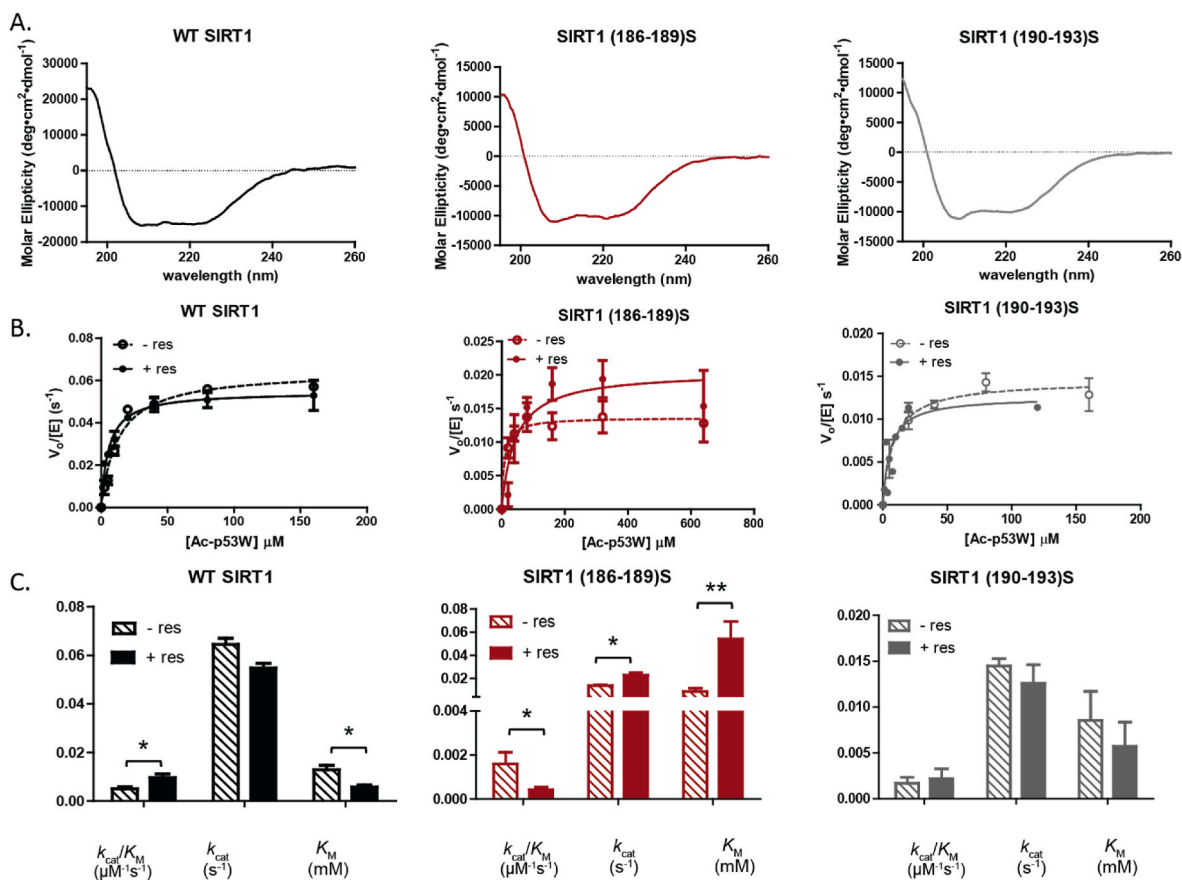|	T186	F187	V188	Q189	Q190	H191	L192	M193
IsUnstruct	0.167	0.138	0.135	0.147	0.148	0.139	0.128	0.131
V_{kabat}	7.500	6.429	6.429	5.000	5.625	5.625	6.429	6.429
E6	0.703	0.668	0.532	0.541	0.526	0.556	0.604	0.627
	T186S	**F187S**	**V188S**	**Q189S**	**Q190S**	**H191S**	**L192S**	**M193S**
IsUnstruct	0.850	0.852	0.842	0.816	0.659	0.678	0.680	0.664
V_{kabat}	2.500	4.091	5.000	5.625	5.000	4.500	2.500	2.308
E6	0.671	0.641	0.511	0.520	0.516	0.555	0.616	0.628

Fig. 2. A. CD spectra of hSIRT1-143 constructs at 25 °C. **B.** Enzyme kinetics and **C.** Michaelis-Menten parameters for different constructs of hSIRT1-143 activity against Ac-p53W with and without the addition of 200 μM resveratrol. All kinetics data were collected in at least triplicates and fit with Graphpad Prizm. Error bars indicate standard error of fit. * depicts $p < 0.05$, ** depicts $p < 0.005$.
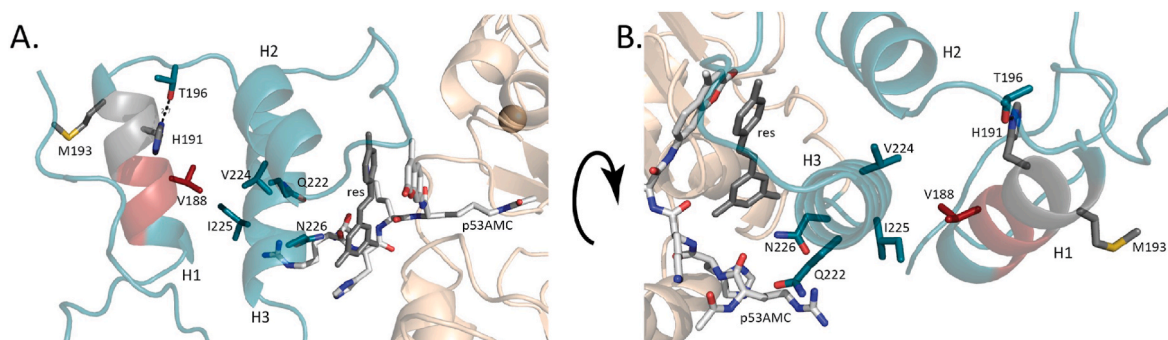

Fig. 3. The SBD (teal) region of SIRT1 (5BTR) showing interactions between key residues in the 186–193 region (red and gray) and the rest of the SBD. The catalytic core is shown in tan. **A.** is the side view of the SBD helices, highlighting the interactions between H191 and T196. **B.** highlights the interaction between V188 and H3 residues. (For interpretation of the references to colour in this figure legend, the reader is referred to the Web version of this article.)

all the existing hSIRT1 structures that include the SBD, H191 is within hydrogen bonding distance of T196, a residue in the loop region connecting H1 to H2 (Fig. 3). Mutating H191 to a serine would disrupt this hydrogen bonding interaction, and again possibly destabilize the three-helix bundle, leading to the decrease in catalytic rate.

Upon addition of resveratrol, the activity of hSIRT1-143 (186–189)S decreased, mainly through an over 6-fold increase in K_M (Fig. 2B and C and Table 2). It is worth noting that V224 and I225, the residues that interact with V188, are on the opposite side of Q222 and N226 in H3, two residues that have been shown to directly interact with resveratrol [17]. The serine mutation at V188 could possibly interrupt the interactions between H3 and resveratrol, which would change the way resveratrol binds to hSIRT1. This result suggested that the mutant still had an allosteric network, but it now behaved in an opposite fashion compared to the wild-type enzyme.

While the 186–189 mutation seemed to affect the allosteric network in an unusual way that was difficult to interpret, the activity of hSIRT1-143 (190–193)S, however, showed no significant change upon the addition of resveratrol (Fig. 2B and C and Table 2). This suggested that the allosteric switch-like region is possibly within these residues.

3.3. Pinpointing M193 as a switch-like residue

From the mutation results above, we concluded that the switch-like region was more likely within residues 190–193. When comparing the secondary structure of these four residues amongst the known SIRT1 structures in the Protein Data Bank (PDB 5BTR, 4ZZH, 4ZZJ, 4ZZI), we found that these residues were part of an α-helical conformation in all structures except for M193 in 4ZZJ, where it was assigned as an undefined structure. This suggested that M193 is possibly the residue that is essential for the allosteric conformational change. To test this hypothesis, we mutated M193 to alanine, then expressed and purified the hSIRT1-143 M193A construct. Sequence descriptor values for the M193A mutation shows limited changes with respect to WT for IsUnstruct values but a moderate increase in the V_{kabat} value of 7.5 (Table S5). This construct still well-folded (Fig. 4A and Table S2) with a melting temperature of 49.4 °C (Table 2 and Fig. S5). Unsurprisingly, the single point mutant recovered some activity against Ac-p53W compared to the four-serine mutants, with a k_{cat} closer to that of WT hSIRT1-143 (Table 2). Addition of resveratrol had little effect on the overall activity of hSIRT1-143 M193A and no significant effect on its substrate recognition (K_M) (Fig. 4B and C and Table 2). This is consistent with our hypothesis that M193 is a crucial residue for the allosteric regulation of

hSIRT1 by resveratrol.

4. Discussion

In this study we successfully predicted and confirmed an allosteric switch-like region using sequence-based indicators in combination with experimental methods and narrowed down the region to a single residue with help from secondary structure comparison. Thus we were able to decouple the allosteric and catalytic functions of a two-domain enzyme by mutating one amino acid, M193 to an alanine. It is important to note that the hSIRT1-143 (186–189)S mutant retains enzyme activity but also shows allosteric regulation by resveratrol, albeit in an opposite fashion. This gives us confidence that the additional secondary structure alignment and experimental confirmations were essential for identifying true allosteric switch-like regions. M193 is distal to any residues with direct interactions with resveratrol, and the mutant construct still binds to resveratrol. This suggests that the lack of allosteric effect is more likely due to the abolishment of allosteric communication, and not the loss of binding between resveratrol and the enzyme. In addition, there are no obvious interactions between M193 and other residues within any of the known hSIRT1 structures (Fig. 4D). This would suggest that M193 controls the allosteric communication via a more global, ensemble motion [6,10] rather than direct interactions. Initial probing with AlloSigMa [47] estimates that once M193 is mutated to a smaller residue, the dynamics of some residues close to the active site are no longer affected when resveratrol binds, which agrees with our experimental results (Fig. S9). As M193 is at the C-terminus end of H1, it is also possible that the mutation is affecting the stability of the α-helix [48]. Here we propose a general model for the M193A mutation's response to resveratrol as outlined in Fig. 4E: Upon the addition of resveratrol, wild type hSIRT1 undergoes a conformational change into a more stable state, likely resulting in better recognition of the acetylated substrate peptide, as suggested by the dominant change in K_M seen in our work (Table 2) and in previous literature. The mutation of the switch-like residue 193 from methionine to alanine disrupts the allosteric network. Whereas the M193A mutant is still catalytically active, it no longer experiences significant change in conformational dynamics when resveratrol is bound due to a disruption in the allosteric network, resulting in no change in the enzyme's catalytic efficiency.

In this work we show a novel method for identifying allosteric switch-like regions within a multidomain enzyme. This newly identified switch-like region could shed light on the allosteric regulation mechanism for hSIRT1. This work also has broader implications for understanding allosteric regulation in general. The position of M193 with no immediate internal interactions with other side chains cautions that allosteric switch-like residues could occur in unexpected regions in proteins. The identification of M193 relies on the fact that the prediction method used in this study examines sequence information in a direct fashion without significant assumptions. Other routes for predicting allosteric switch-like regions tend to either require extensive structural information [10] or are more computationally and statistically demanding, using methods such as Molecular Dynamics (MD), community network analysis [13] and statistical coupling analysis (SCA) [12]. The method used in this study is more accessible, it can be easily scaled up to screen large numbers of proteins, and can be broadly applied to solve complex problems in terms of allosteric regulation.

Declaration of interests

Table 2
Melting temperature and Michaelis-Menten kinetics parameters of WT and mutant hSIRT1-143 constructs against Ac-p53W with and without the addition of 200 μM resveratrol. All enzyme kinetics data were obtained in triplicates. The T_M and Michaelis-Menten parameters were fit with GraphPad Prism and the standard errors of fit are included.

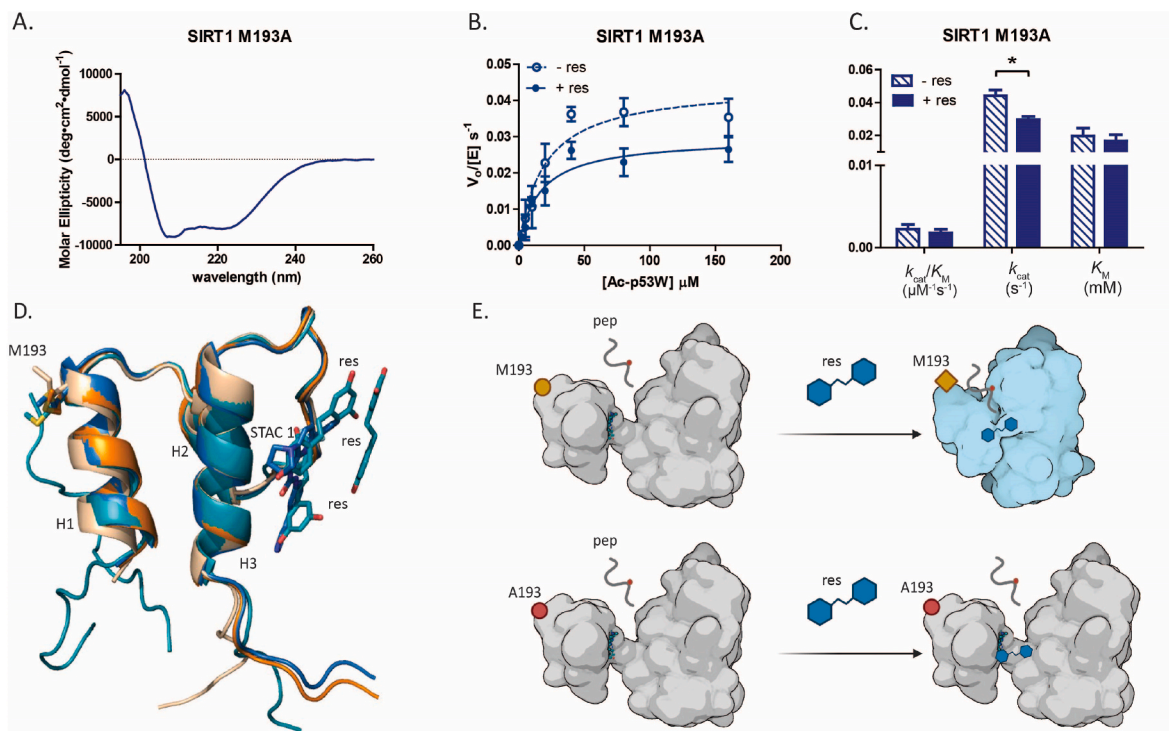|	T_M (°C)	Resveratrol	k_{cat} (s^{-1})	K_M (μM)	k_{cat}/K_M (μM^{-1}s^{-1})
WT hSIRT1-143	54 ± 1.3	–	0.06 ± 0.003	13 ± 1.8	0.005 ± 0.0007
		+	0.056 ± 0.002	6 ± 0.9	0.010 ± 0.0015
hSIRT1-143 (186–189)S	47 ± 1.5	–	0.01 ± 0.0006	9 ± 2.8	0.0016 ± 0.0005
		+	0.02 ± 0.002	54 ± 15.1	0.0004 ± 0.00012
hSIRT1-143 (190–193)S	48 ± 0.6	–	0.01 ± 0.0008	9 ± 3.2	0.0017 ± 0.00064
		+	0.01 ± 0.002	6 ± 2.6	0.0022 ± 0.00106
hSIRT1-143 M193A	49 ± 0.6	–	0.04 ± 0.003	20 ± 4.8	0.0022 ± 0.00058
		+	0.03 ± 0.002	17 ± 3.9	0.0018 ± 0.00044

Fig. 4. A. CD spectra of hSIRT1-143 M193A at 25 °C. **B.** Enzyme kinetics and **C.** Michaelis-Menten parameters for hSIRT1-143 M193A activity against Ac-p53W with and without the addition of 200 μM resveratrol. All kinetics data were collected in triplicates and fit with Graphpad Prizm. Error bars indicate standard error of fit. * depicts p < 0.05. **D.** Overlay of the SBD from PDB structures 5BTR (teal); 4ZZH (blue); 4ZZI (tan); 4ZZJ (orange) showing the position of M193 relative to SIRT1 modulators such as resveratrol (teal) and STAC 1 (blue). **E.** Proposed model for the response of SIRT1 to resveratrol before and after the M193A mutation. Created with BioRender.com. (For interpretation of the references to colour in this figure legend, the reader is referred to the Web version of this article.)

Data availability

Data will be made available on request.

Appendix A. Supplementary data

Supplementary data to this article can be found online at https://doi.org/10.1016/j.bbrep.2022.101275.

References

[1] J.-P. Changeux, Allostery and the Monod-Wyman-Changeux model after 50 years, Annu. Rev. Biophys. 41 (2012) 103–133.
[2] N.M. Goodey, S.J. Benkovic, Allosteric regulation and catalysis emerge via a common route, Nat. Chem. Biol. 4 (2008) 474–482.
[3] K. Gunasekaran, B. Ma, R. Nussinov, Is allostery an intrinsic property of all dynamic proteins? Proteins Struct. Funct. Genet. 57 (2004) 433–443.
[4] J.-P. Changeux, A. Christopoulos, Allosteric modulation as a unifying mechanism for receptor function and regulation, Cell 166 (2016) 1084–1102.
[5] D. Kern, E.R. Zuiderweg, The role of dynamics in allosteric regulation, Curr. Opin. Struct. Biol. 13 (2003) 748–757.
[6] C.A. Smith, D. Ban, S. Pratihar, K. Giller, M. Paulat, S. Becker, C. Griesinger, D. Lee, B.L. De Groot, Allosteric switch regulates protein-protein binding through collective motion, Proc. Natl. Acad. Sci. U. S. A. 113 (2016) 3269–3274.
[7] H.N. Motlagh, J.O. Wrabl, J. Li, V.J. Hilser, The ensemble nature of allostery, Nature 508 (2014) 331–339.
[8] R.H. Bekendam, P.K. Bendapudi, L. Lin, P.P. Nag, J. Pu, D.R. Kennedy, A. Feldenzer, J. Chiu, K.M. Cook, B. Furie, M. Huang, P.J. Hogg, R. Flaumenhaft, A substrate-driven allosteric switch that enhances PDI catalytic activity, Nat. Commun. 7 (2016) 1–11.
[9] S. Vahidi, Z.A. Ripstein, J.B. Juravsky, E. Rennella, A.L. Goldberg, A.K. Mittermaier, J.L. Rubinstein, L.E. Kay, An allosteric switch regulates Mycobacterium tuberculosis ClpP1P2 protease function as established by cryo-EM and methyl-TROSY NMR, Proc. Natl. Acad. Sci. U. S. A. 117 (2020) 5895–5906.
[10] N. Sharma, N. Ahalawat, P. Sandhu, E. Strauss, J. Mondal, R. Anand, Role of allosteric switches and adaptor domains in long-distance cross-talk and transient tunnel formation, Sci. Adv. 6 (2020), eaay7919.
[11] D. Kovacs, B. Szabo, R. Pancsa, P. Tompa, Intrinsically disordered proteins undergo and assist folding transitions in the proteome, Arch. Biochem. Biophys. (2013).
[12] W. Jiao, Y. Fan, N.J. Blackmore, E.J. Parker, A single amino acid substitution uncouples catalysis and allostery in an essential biosynthetic enzyme in Mycobacterium tuberculosis, J. Biol. Chem. 295 (2020) 6252–6262.
[13] L.G. Ahuja, A.P. Kornev, C.L. Mcclendon, G. Veglia, S.S. Taylor, Mutation of a kinase allosteric node uncouples dynamics linked to phosphotransfer, Proc. Natl. Acad. Sci. U. S. A. 114 (2017) E931–E940.
[14] J. Wang, H. Fivecoat, L. Ho, Y. Pan, E. Ling, G.M. Pasinetti, The role of Sirt1: at the crossroad between promotion of longevity and protection against Alzheimer's disease neuropathology, Biochim. Biophys. Acta Protein Proteonomics 1804 (2010) 1690–1694.
[15] X. Qiu, K.V. Brown, Y. Moran, D. Chen, Sirtuin regulation in calorie restriction, Biochim. Biophys. Acta Protein Proteonomics 1804 (2010) 1576–1583.
[16] J. Yi, J. Luo, SIRT1 and p53, effect on cancer, senescence and beyond, Biochim. Biophys. Acta Protein Proteonomics 1804 (2010) 1684–1689.
[17] D. Cao, M. Wang, X. Qiu, D. Liu, H. Jiang, N. Yang, R.-M. Xu, Structural basis for allosteric, substrate-dependent stimulation of SIRT1 activity by resveratrol, Genes Dev. 29 (2015) 1316–1325.
[18] J.L. Feldman, K.E. Dittenhafer-Reed, J.M. Denu, Sirtuin catalysis and regulation, J. Biol. Chem. 287 (2012) 42419–42427.
[19] A.M. Davenport, F.M. Huber, A. Hoelz, Structural and functional analysis of human SIRT1, J. Mol. Biol. 426 (2014) 526–541.
[20] B.D. Sanders, B. Jackson, R. Marmorstein, Structural basis for sirtuin function: what we know and what we don't, Biochim. Biophys. Acta Protein Proteonomics 1804 (2010) 1604–1616.
[21] M. Pan, H. Yuan, M. Brent, E.C. Ding, R. Marmorstein, SIRT1 contains N- and C-terminal regions that potentiate deacetylase activity, J. Biol. Chem. 287 (2012) 2468–2476.

[22] R. Meledin, A. Brik, A. Aharoni, Dissecting the roles of the N- and C-flanking residues of acetyllysine substrates for SIRT1 activity, Chembiochem 14 (2013) 577–581.

[23] H. Dai, D.A. Sinclair, J.L. Ellis, C. Steegborn, Sirtuin activators and inhibitors: promises, achievements, and challenges, Pharmacol. Ther. 188 (2018) 140–154.

[24] H. Kang, J.Y. Suh, Y.S. Jung, J.W. Jung, M.K. Kim, J.H. Chung, Peptide switch is essential for Sirt1 deacetylase activity, Mol. Cell. 44 (2011) 203–213.

[25] H. Dai, A.W. Case, T.V. Riera, T. Considine, J.E. Lee, Y. Hamuro, H. Zhao, Y. Jiang, S.M. Sweitzer, B. Pietrak, B. Schwartz, C.A. Blum, J.S. Disch, R. Caldwell, B. Szczepankiewicz, C. Oalmann, P. Yee Ng, B.H. White, R. Casaubon, R. Narayan, K. Koppetsch, F. Bourbonais, B. Wu, J. Wang, D. Qian, F. Jiang, C. Mao, M. Wang, E. Hu, J.C. Wu, R.B. Perni, G.P. Vlasuk, J.L. Ellis, Crystallographic structure of a small molecule SIRT1 activator-enzyme complex, Nat. Commun. 6 (2015) 7645.

[26] F. Ghisays, C.S. Brace, S.M. Yackly, H.J. Kwon, K.F. Mills, E. Kashentseva, I. P. Dmitriev, D.T. Curiel, S. Imai, T. Ellenberger, The N-terminal domain of SIRT1 is a positive regulator of endogenous SIRT1-dependent deacetylation and transcriptional outputs, Cell Rep. 10 (2015) 1665–1673.

[27] D.A. Sinclair, L. Guarente, Small-molecule allosteric activators of sirtuins, Annu. Rev. Pharmacol. Toxicol. 54 (2014) 363–380.

[28] R. Nepal, J. Spencer, G. Bhogal, A. Nedunuri, T. Poelman, T. Kamath, E. Chung, K. Kantardjieff, A. Gottlieb, B. Lustig, Logistic regression models to predict solvent accessible residues using sequence-and homology-based qualitative and quantitative descriptors applied to a domain-complete X-ray structure learning set, J. Appl. Crystallogr. 48 (2015) 1976–1984.

[29] M. Young, K. Kirshenbaum, K.A. Dill, S. Highsmith, Predicting conformational switches in proteins, Protein Sci. 8 (1999) 1752–1764.

[30] S. Mishra, L.L. Looger, L.L. Porter, Inaccurate secondary structure predictions often indicate protein fold switching, Protein Sci. 28 (2019) 1487–1493.

[31] M. Bodén, T.L. Bailey, Identifying sequence regions undergoing conformational change via predicted continuum secondary structure, Bioinformatics 22 (2006) 1809–1814.

[32] R. Adamczak, A. Porollo, J. Meller, Combining prediction of secondary structure and solvent accessibility in proteins, Proteins Struct. Funct. Bioinforma. 59 (2005) 467–475.

[33] B. Strauss, Predicting Switch-like Behavior in Proteins Using Logistic Regression on Sequence-Based Descriptors, San Jose State University, 2019.

[34] M.Y. Lobanov, I.V. Sokolovskiy, O.V. Galzitskaya, IsUnstruct: prediction of the residue status to be ordered or disordered in the protein chain by a method based on the Ising model, J. Biomol. Struct. Dyn. 31 (2013) 1034–1043.

[35] K.M. Saravanan, S. Selvaraj, Performance of secondary structure prediction methods on proteins containing structurally ambivalent sequence fragments, Biopolymers 100 (2013) 148–153.

[36] L.A. Mirny, E.I. Shakhnovich, Universally conserved positions in protein folds: reading evolutionary signals about stability, folding kinetics and function, J. Mol. Biol. 291 (1999) 177–196.

[37] B.C. Smith, W.C. Hallows, J.M. Denu, A continuous microplate assay for sirtuins and nicotinamide-producing enzymes, Anal. Biochem. 394 (2009) 101–109.

[38] C. Louis-Jeune, M.A. Andrade-Navarro, C. Perez-Iratxeta, Prediction of protein secondary structure from circular dichroism using theoretically derived spectra, Proteins Struct. Funct. Bioinforma. 80 (2012) 374–381.

[39] H. Liao, W. Yeh, D. Chiang, R.L. Jernigan, B. Lustig, Protein sequence entropy is closely related to packing density and hydrophobicity, Protein Eng. Des. Sel. 18 (2005) 59–64.

[40] M.Y. Lobanov, O. V Galzitskaya, The Ising model for prediction of disordered residues from protein sequence alone, Phys. Biol. 8 (2011), 035004.

[41] J.G. Graham, B. Lustig, Computational Characterization of Sequences with Multiple Conformational Propensities in the Sirtuin Family of NAD+-dependent Histone Deacetylases, 2018.

[42] M.T. Borra, B.C. Smith, J.M. Denu, Mechanism of human SIRT1 activation by resveratrol, J. Biol. Chem. 280 (2005) 17187–17195.

[43] M. Lakshminarasimhan, U. Curth, S. Moniot, S. Mosalaganti, S. Raunser, C. Steegborn, Molecular architecture of the human protein deacetylase Sirt1 and its regulation by AROS and resveratrol, Biosci. Rep. 33 (2013) 395–404.

[44] O. Trott, A.J. Olson, AutoDock Vina, Improving the speed and accuracy of docking with a new scoring function, efficient optimization, and multithreading, J. Comput. Chem. 31 (2010) 455–461.

[45] V. Modi, D. Lama, R. Sankararamakrishnan, Relationship between helix stability and binding affinities: Molecular dynamics simulations of Bfl-1/A1-binding pro-apoptotic BH3 peptide helices in explicit solvent, J. Biomol. Struct. Dyn. (2013) 65–77.

[46] T.C. Krzysiak, L. Thomas, Y.-J. Choi, S. Auclair, Y. Qian, S. Luan, S.M. Krasnow, L. L. Thomas, L.M.I. Koharudin, P.V. Benos, D.L. Marks, A.M. Gronenborn, G. Thomas, An insulin-responsive sensor in the SIRT1 disordered region binds DBC1 and PACS-2 to control enzyme activity, Mol. Cell. 72 (2018).

[47] Z.W. Tan, E. Guarnera, W.V. Tee, I.N. Berezovsky, AlloSigMA 2: paving the way to designing allosteric effectors and to exploring allosteric effects of mutations, Nucleic Acids Res. 48 (2020) W116–W124.

[48] D. Sitkoff, D.J. Lockhart, K.A. Sharp, B. Honig, Calculation of electrostatic effects at the amino terminus of an alpha helix, Biophys. J. 67 (1994) 2251–2260.